Copurification of the FpvA Ferric Pyoverdin Receptor of *Pseudomonas aeruginosa* with Its Iron-Free Ligand: Implications for Siderophore-Mediated Iron Transport†

Isabelle J. Schalk,*,‡ Pavel Kyslik,§ Danielle Prome,|| Alain van Dorsselaer,⊥ Keith Poole,# Mohamed A. Abdallah,‡ and Franc Pattus‡

Département des Récepteurs et Protéines Membranaires, UPR 9050 CNRS, ESBS, Bld Sébastien Brant, F-67 400 Illkirch, Strasbourg, France, Institute of Microbiology, Academy of Sciences of the Czech Republic, Vídenská 1083, 142 20 Prague 4, Czech Republic, Signaux Biologiques et Spectrométrie de Masse, Institut de Pharmacologie et de Biologie Structurale, 31 077 Toulouse Cedex, France, Laboratoire de Spectrométrie de Masse Bio-organique, associé au CNRS, Faculté de Chimie, 1 rue Blaise Pascal, 67 008 Strasbourg Cedex, France, and Department of Microbiology and Immunology, Queen's University, Kingston, Ontario, Canada K7L 3N6

Received February 22, 1999; Revised Manuscript Received May 5, 1999

ABSTRACT: The *Pseudomonas aeruginosa* FpvA receptor is a TonB-dependent outer membrane transport protein that catalyzes uptake of ferric pyoverdin across the outer membrane. Surprisingly, FpvA expressed in *P. aeruginosa* grown in an iron-deficient medium copurifies with a ligand X that we have characterized by UV, fluorescence, and mass spectrometry as being iron-free pyoverdin (apo-PaA). PaA was absent from FpvA purified from a PaA−deficient *P. aeruginosa* strain. The properties of ligand binding in vitro revealed very similar affinities of apo-PaA and ferric−PaA to FpvA. Fluorescence resonance energy transfer was used to study in vitro the formation of the FpvA−PaA−Fe complex in the presence of PaA−Fe or citrate−Fe. The circular dichroism spectrum of FpvA indicated a 57% β-structure content typical of porins and in agreement with the 3D structures of the siderophore receptors FhuA and FepA. In the absence of the protease's inhibitors, a truncated form of FpvA lacking 87 amino acids at its N-terminus was purified. This truncated form still bound PaA, and its β-sheet content was conserved. This N-terminal region displays significant homology to the N-terminal periplasmic extensions of FecA from *Escherichia coli* and PupB from *Pseudomonas putida*, which were previously shown to be involved in signal transduction. This suggests a similar function for FpvA. The mechanism of iron transport in *P. aeruginosa* via the pyoverdin pathway is discussed in the light of all these new findings.

In response to iron deprivation, *Pseudomonas aeruginosa* synthesizes at least two known siderophores, pyoverdin (*1*) and pyochelin (*2*), characterized by completely different structures, physiochemical properties, and affinities for Fe(III). These systems operate both in the organism's natural habitat, soil and water, where the solubility of iron at neutral pH is extremely low, and in the human host where the availability of free iron is too low to sustain bacterial growth [due to the iron-binding glycoproteins transferrin and lactoferrin (*3*)].

Pyochelin is a phenolate compound that exhibits a relatively low affinity for iron in vitro (*2*, *4*). Pyoverdin, the major endogenous siderophore, possesses a chromophore derived from 2,3-diamino-6,7-dihydroxyquinoline that confers color and fluorescence to the molecule, linked to a partly cyclic octapeptide (*5*, *6*). The peptide differs among strains by the number, composition, and configuration of amino acids. A third constituent of the molecule, usually formed by a succinamide group linked to the amino group at position C-3 of the chromophore, can also differ depending on the strain. Iron(III) is strongly chelated by the cathecolate group of the quinoline moiety and the two hydroxamate groups of the two δ-*N*-hydroxyornithines of the octapeptide. The stability constant is approximately 10^{24} M^{-1} at neutral pH (*5*, *7*).

The mechanism usually proposed for the transport of ferric siderophores into Gram-negative bacterial cells is comprised of a number of steps. Initially the iron-containing siderophore is recognized by a specific outer membrane receptor. The activity of this siderophore receptor is dependent on the energy input that is provided by the proton motive force of the cytoplasmic membrane. Energy is transmitted from the cytoplasmic membrane to the outer membrane by a complex that consist of the three proteins TonB, ExbB, and ExbD, of which TonB and ExbD are located in the periplasm between the cytoplasmic membrane and the outer membrane with their NH_2 termini inserted in the cytoplasmic membrane (*8*−*10*). Somehow, TonB transduces its conformationally stored

† This work was funded by the Centre National de la Recherche Scientifique (Program Physique et Chimie du Vivant), the Ministère de l'Enseignement Supérieur, de la Recherche et de la Technologie (ACC-SDV5), and the Medical Research Council of Canada. K.P. is a Natural Sciences and Engineering Research Council of Canada University Research Fellow.

* To whom correspondence should be addressed. E-mail: schalk@esbs.u-strasbg.fr. Phone: (33) 03 88 65 52 73. Fax: (33) 03 88 65 52 98.

‡ UPR 9050 CNRS.

§ Academy of Sciences of the Czech Republic.

|| Institut de Pharmacologie et de Biologie Structurale.

⊥ Laboratoire de Spectrométrie de Mass Bio-organique.

Queen's University.

10.1021/bi990421x CCC: $18.00
Published on Web 06/30/1999

energy to the outer membrane receptor, and ferric siderophores are pumped against their gradients across the outer membrane. From there, it has been shown in *Escherichia coli* that the ferric siderophores are picked up by binding proteins and actively transported across the cytoplasmic membrane by conventional ABC transporters in a TonB-independent fashion.

The *P. aeruginosa* outer membrane receptor for ferric pyoverdin is a 86 kDa protein encoded by the *fpvA* gene (*11*, *12*). The expression of this receptor is regulated positively by pyoverdin (*13*) and negatively by the iron concentration in the growth medium. The FpvA product belongs to the siderophore outer membrane receptor family and shows homology to the ferric pseudobactin receptors PupA and PupB of *Pseudomonas putida* and the coprogen/rhodotorulic acid receptor FhuE of *E. coli* (*12*). The X-ray structure of FhuA and FepA (respectively the *E. coli* ferrichrome−iron and enterobactin−iron receptors) have been reported recently (*14*−*16*). Both receptors are composed of a COOH-terminal β-barrel domain and an NH_2-terminal cork domain, which fills the barrel interior. In the FhuA−ferrichrome−iron X-ray structure (*14*, *15*), the ferrichrome−iron is fixed above the cork well outside the membrane by hydrogen bounds and van der Waals contacts, in a binding site formed by eight aromatic residues and one residue each of Arg, Glu, and Gly. The key differences between the structures of FhuA and its complex with ferrichrome−iron are localized in the cork domain, especially a helix termed the switch helix that is located in the periplasm pocket in the ligand-free conformation which is completely unwound in the FhuA−ferrichrome−iron complex. But despite the X-ray data of FhuA, FhuA−ferrichrome-iron, and FepA, the mechanism of siderophore−iron transport through the outer membrane remains unsolved. In vivo and in vitro electron spin resonance spectroscopy showed a ferric-enterobactin-induced conformational change in FepA (*17*, *18*). These changes were not merely associated with ferrisiderophore binding but occurred during its uptake through the outer membrane and may reflect a change of the conformation of FepA.

In this paper we describe the unexpected copurification of the *P. aeruginosa* outer membrane receptor FpvA with a tightly bound ligand which was absent when the receptor was purified from a pyoverdin-deficient strain. This ligand was found to be the iron-free form of the siderophore pyoverdin (apo-PaA)[1].

MATERIALS AND METHODS

Chemicals. The detergents used included Zwittergent 3-14 (3-(*N*,*N*-dimethylmyristylammonio)propanesulfonate) from Fluka (Buchs, Switzerland) and octyl-POE (*N*-octylpoly-(oxyethylene)) from Bachem (Basel, Switzerland). Q-Sepharose Fast Flow anion-exchange resin was obtained from Pharmacia (Uppsala, Sweden). Lysozyme, DNAse, RNAse, and the protease's inhibitors (cocktail tablets) were purchased from Boehringer Mannheim (Mannheim, Germany). The sodium *N*-laurylsarcosinate (sarkosyl) was from Sigma (Buchs, Switzerland).

[1] Abbreviations: apo-PaA, iron-free pyoverdin; PaA−Fe, ferric pyoverdin.

Bacterial Strains, Plasmids, and Growth Media. P. aeruginosa strain K691 is a FpvA−deficient mutant whose construction is described below. The PaA−deficient *P. aeruginosa* strain CDC5 was originally described by Ankenbauer et al. (*19*). The mutation has been mapped on the pvd locus which contains genes involved in the synthesis of the peptide moiety of pyoverdin. Overproduction of FpvA in K691 and CDC5 strains was achieved by introduction of plasmid pPVR2. Strains CDC5(pPVR2) and K691(pPVR2) were grown under aerobic conditions in a succinate medium (*6*) in the presence of 100 μg/mL tetracycline and 200 μg/mL carbenicillin for strain K691(pPVR2) and in the presence of 200 μg/mL carbenicillin for strain CDC5(pPVR2).

P. aeruginosa PAO1, a wild-type strain, was used in the construction of the mutant K691 by in vitro mutagenesis and gene replacement. *E. coli* DH5α (*20*) has been described previously. Plasmid pPVR2 is a derivative of the *E. coli*−*P. aeruginosa* shuttle cloning vector pAK1900 carrying the *fpvA* gene on a 4.6 kb *Sph*I insert (*12*). Plasmid pSUP202ΔTc (*21*) is a pSUP202 (*22*) derivative harboring a deletion in the *tet* gene of this vector. Plasmid pHP45ΩTc (*23*) has been described. Due to an instability of the ΩTc insert in K691 in the absence of antibiotic selection, K691 and plasmid-containing derivatives of this strain were always cultured in the presence of tetracycline.

Construction of Strain K691(pPVR2). The tetracycline-resistant derivative of the Ω interposon (ΩTc) present on plasmid pHP45ΩTc was recovered on a ca. 2 kb *Sma*I fragment and inserted into the *Sca*I site of *fpvA* on pPVR2. This necessitated partial digestion of pPVR2 with *Sca*I and isolation of a ca. 9 kb fragment representing a full-length pPVR2. Transformants (*E. coli* DH5α) carrying pPVR2 with a ΩTc insert were selected on L-agar containing ampicillin and tetracycline, and insertion of the ΩTc within the *fpvA* gene was assessed by restriction analysis. The WTc mutagenized *fpvA* gene was subsequently recovered on a ca. 6.5 kb *Pst*I fragment and cloned into the unique *Pst*I site on plasmid pSUP202ΔTc. Following introduction into *E. coli* strain S17-1, the vector was mobilized into *P. aeruginosa* PAO1 via conjugation (*21*). *P. aeruginosa* PAO1 strain used for this conjugation is a derivative carrying a chromosomal *fpvA*::ΩTc mutation, selected on L-agar containing tetracycline and screened for the absence of plasmid-encoded carbenicillin resistance. The lack of FpvA in these putative mutants was confirmed by SDS−polyacrylamide gel electrophoresis of isolated outer membranes.

Purification of Pyoverdin. Pyoverdin was prepared as described previously (*6*, *7*). Pyoverdin concentrations were determined spectrophotometrically using the molar extinction coefficient of $\epsilon_{380\ nm} = 16\,500\ M^{-1}$ and $\epsilon_{400\ nm} = 19\,000\ M^{-1}$ for the PaA and the PaA−Fe forms respectively (*6*, *24*).

Purification of FpvA and FpvA−*X.* Strains K691 carrying the cloned *fpva* gene on the multicopy plasmid pPVR2 and CDC5(pPVR2) were used for the purification of FpvA−X and FpvA, respectively. Both strains produce FpvA, but CDC5(pPVR2) does not produce pyoverdin. The first step of purification in both cases involved preparation of outer membranes as described (*25*, *26*) with some modifications. The bacteria pellets were resuspended in 50 mM Tris-HCl pH 8.0 in the presence of 1 mg/mL lysozyme, 1 mg/mL RNAse, 1 mg/mL DNAse, and the protease's inhibitors (cocktail tablets, 1 tablet per 50 mL). The cells were disrupted

by two passages through a French pressure cell (15 000 lb/in^2). Incubation of the mixture for 15 min at 37 °C with 2% (w/v) sodium *N*-laurylsarcosinate (sarkosyl) solubilized the cytoplasmic membranes, leaving the outer membrane intact. Outer membranes were pelleted by centrifugation at 20 000*g* for 1 h. The pellets were extracted five times at room temperature with 50 mM Tris-HCl pH 8.0 and 1% (w/v) Zwittergent 3-14 in the presence of the protease's inhibitors (cocktail tablets, 1 tablet per 50 mL). The solubilized protein fractions were dialyzed against 50 mM Tris-HCl pH 8.0 and 1% (v/v) octyl-POE (buffer A) and applied to a Q-Sepharose Fast Flow column (30 cm × 1 cm) equilibrated with buffer A. The column was washed with 20 mL of buffer A and eluted with a linear gradient of 0−500 mM NaCl in buffer A. A final purification was achieved on the same Q-Sepharose column equilibrated with 50 mM potassium phosphate buffer pH 6.8 and 1% octyl-POE (buffer B). A linear gradient of 0−500 mM NaCl in buffer B was applied, and the fractions containing FpvA or FpvA-X were concentrated by ultra filtration using Amicon YM10 membranes. The purified protein concentration was determined using the molar extinction coefficient at 280 nm (158 740 M^{-1}, determined from the amino acid sequence) of FpvA. The purification of FpvA was monitored at each step by SDS−PAGE and Western's blots using an anti-FpvA antiserum prepared as described by Poole et al. (*12*).

FpvA-X and Truncated FpvA−X (tFpvA−X) N-Terminal Amino Acid Micro Sequence Analysis. Automated Edman degradations on FpvA−X and tFpvA−X were performed on an amino acid sequencer (Applied Biosystems, model 473A) in the liquid pulse mode (Perkin-Elmer, Applied Biosystem Division, Foster city, CA).

Isolation, Purification, and Characterization of Ligand X Copurified with FpvA. A 50 mL volume of purified FpvA−X (0.5 mg/mL) was dialyzed against H_2O and then denatured at pH 2.0 by the addition of trifluoroacetic acid (TFA). Protein denaturation was followed by fluorescence measurements (see fluorescence below). X was separated from FpvA by filtration on a centricon filter (Macrosep, 10K), and the solution of molecule X was concentrated to a volume of 500 μL using a Speed-Vac instrument. The remaining octyl-POE was removed by two successive MeOH/$CHCl_3$ (2:1) extractions. Ligand X was further purified by reverse-phase HPLC on a column (Nucleosil ODS 5u SIN, Jones Chromatography) as described for PaA and PaA−Fe by Albrecht-Gary et al. (*7*).

Electrophoretic analysis of X and PaA on cellulose acetate membranes (Midifilm, Biomidi) was carried out using a horizontal electrophoresis tank as described (*7*). Electrophoresis was performed in 100 mM pyridine−acetic acid pH 5.0 at a constant voltage (300 V) for 30 min.

The stoichiometry of iron binding to X and PaA was determined as described by Meyer and Abdallah (*27*). To 1 mL of X in 50 mM pyridine−acetic acid pH 5.0 (6.1 μM, $\epsilon = 16\,500\ M^{-1}$ at 380 nm), stepwise additions (2.7 μL) of a freshly prepared aqueous solution of 0.21 μM $FeCl_3$ in 0.5 N HCl were made. The saturation curve was monitored by following the appearance of an absorption at 450 nM, and the stoichiometry was deduced using the extinction coefficient of PaA−Fe ($\epsilon = 6800\ M^{-1}$ at 450 nm).

Ligand Binding Assays. For the determination of the dissociation constant of PaA−^{55}Fe from FpvA in vitro, and for the competition experiments with apo-PaA, we used the filtration assay developed for detergent-solubilized G-coupled receptors (GPCR) (*28*−*30*). In brief, purified FpvA from strain CDC5(pPVR2) (8 nM) was incubated in a total volume of 500 μL of 50 mM Tris-HCl pH 8.0 and 1% (w/v) octyl-POE at room temperature for 2 h in the presence of varying concentrations of PaA−^{55}Fe (0.5−800 nM). The solution of PaA complexed to ^{55}Fe (from $^{55}FeCl_3$, specific activity of 3 Ci/g, NEN, Boston, MA) was prepared using a 260 μM solution of PaA in water. To 77 μL of this solution was added 48 μL of a solution of $^{55}FeCl_3$ (3 mCi/g), obtained by dilution of the stock solution, plus 875 μL of 50 mM Tris-HCl pH 8.0 and 1% (v/v) octyl-POE. For competition experiments, purified FpvA (8 nM, 500 μL final volume) was incubated at room temperature for 2 h with PaA−^{55}Fe (12 nM) and various concentrations of unlabeled PaA (0.1−1500 nM) or PaA−Fe (0.1−1500 nM). Incubations were stopped by filtering the assay mixtures over GF/B filters (Whatman), which were rapidly washed three times with 3 mL of 50 mM Tris-HCl pH 8.0 and counted for radioactivity in a scintillation cocktail. The filters were presoaked in 0.1% polyethylenimine to reduce the nonspecific retention of PaA−^{55}Fe.

Apparent binding affinity constants (K_i) of siderophores were calculated from IC_{50} values, determined in competition experiments, according to the Cheng and Prusoff relation (*31*): $K_i = IC_{50}/(1 + L/K_d)$ where L and K_d are respectively the radiolabeled concentration and its equilibrium dissociation constant which was determined experimentally.

The validity for purified FpvA of this filtration assay formerly developed for GPCR was controlled by equilibrium dialysis experiments (data not shown) and was supported by the consistency between the measured B_{max} (the number of bound PaA−Fe at saturation) and the known number of moles of FpvA used in the assay.

Formation of the Iron-Loaded FpvA−X Complex. Purified FpvA−PaA (3.6 μM) from strain K691(pPVR2) was incubated in the presence of 70 μM PaA−Fe or 1 mM citrate−Fe in 3 mL of 50 mM potassium phosphate buffer pH 7.0 and 1% (v/v) octyl-POE at room temperature. At different times 300 μL aliquots of the mixture were applied to a gel filtration column (G50, 15 × 0.5 cm, Pharmacia) in order to separate unbound PaA−Fe or unbound citrate−Fe from the protein. Iron binding was measured after gel filtration by fluorescence measurements (excitation at 290 nm), and the percentage of FpvA−PaA−Fe formed was calculated. Iron binding by FpvA−PaA was evidenced by a decrease in the peak of emission at 447 nm.

Mass Spectrometry. FpvA−PaA and tFpvA−PaA molecular weight determination by MALDI-MS was performed on a time-of-flight Bruker Biflex TM instrument (Bruker, Bremen, Germany) in the linear mode at 19 kV of acceleration potential. FpvA−PaA and tFpvA−PaA were dissolved in CH_3CN/H_2O (1:1), and 2 mL of this solution was mixed with 2 mL of matrix solution (7 mg/mL of a cyano-4-hydroxycinnamic acid in 50:50 acetonitrile/H_2O). Finally, 1 mL was deposited on the target and dried under reduced pressure.

Mass measurements of X and PaA were performed on an Autospec 6F instrument equipped with an electrospray source (Micromass, Altrincham, U.K.). The mobile phase was a mixture of H_2O/methanol (1:1) acidified with 1% acetic acid,

at a flow rate of 10 μL/min. The sampling cone was at 50 eV, and the temperature of the source 80 °C. The samples were dissolved in a mixture of H_2O/methanol (1:1) acidified with 1% acetic acid and injected using a rheodyn injector fitted with a 10 μL loop.

Spectroscopy

Fluorescence. Fluorescence experiments were performed with a SPEX Fluorolog-2 spectrofluorimeter (SPEX Industries, Inc., Edison, NJ). Emission spectra of FpvA were recorded with an excitation wavelength of 290 nm and slit widths of 1 and 4 mm for excitation and emission, respectively, in 50 mM Tris-HCl pH 8.0 and 1% (v/v) octyl-POE. When the effect of urea on the maximum emission wavelengths of tryptophans and of the copurified ligand was studied, samples were incubated for at least 30 min before spectra were recorded. Emission spectra of X and PaA were recorded with an excitation wavelength of 400 nm and the same slit widths as above in 50 mM Tris-HCl pH 8.0.

UV−Visible. Absorption spectra in the visible and ultraviolet regions were performed on a Cary 1E UV−visible double-beam spectrophotometer (Varian Analytical Instruments, Les Ulis, France).

Circular Dichroism. CD analyses were performed with a Jobin Yvon CD6 spectropolarimeter (Jobin-Yvon Instruments SA, Longjumeau, France). Protein samples were placed in a 0.02 cm path-length quartz cuvette for measurements in the far-UV region (185−260 nm). The protein was diluted in 50 mM potassium phosphate buffer pH 6.8 and 1% (v/v) octyl-POE to a concentration of 2.1 μM for FpvA and 2.2 μM for tFpvA−X. Deconvolution of the spectra was done using the Provencher and the VRSL programs (*32*, *33*).

RESULTS

Purification and Characterization of FpvA and FpvA−X. Two *Pseudomonas aeruginosa* strains were used to purify the FpvA receptor, a PaA−producing strain (strain K691, carrying the *fpvA* plasmid pPVR2) and a strain that is unable to produce pyoverdin (strain CDC5(pPVR2)). The first stage of purification was an outer membrane preparation. Zwittergent 3-14 was the best detergent to solubilize the receptor from outer membranes but was then exchanged for octyl-PoE, which does not precipitate at 4 °C and does not interfere with protein concentration assays. Purified proteins were recovered from both strains (6 and 5 mg from respectively 18 L of culture of K691(pPVR2) and CDC5(pPVR2) strains) as judged by SDS−PAGE (Figure 1), Western's blot, N-terminal sequencing, and mass spectrometry measurements. By MALDI-MS, a molecular weight of 86 109 ± 1167 Da was determined for FpvA purified from both strains.

The UV spectrum of FpvA purified from the PaA-producing strain K691(pPVR2) grown in an iron-deficient medium showed that the protein was copurified with a ligand X having a λ_{max} at 400 nm at pH 8.0 (Figure 2A). This copurification was quite evident from fluorescence measurements. When purified FpvA−X was excited at the excitation wavelength of the tryptophans (290 nm), emission peaks at 337 nm and at 447 nm were observed (Figure 2B), corresponding to the fluorescence of the FpvA tryptophans and of molecule X, respectively. At the excitation wavelength

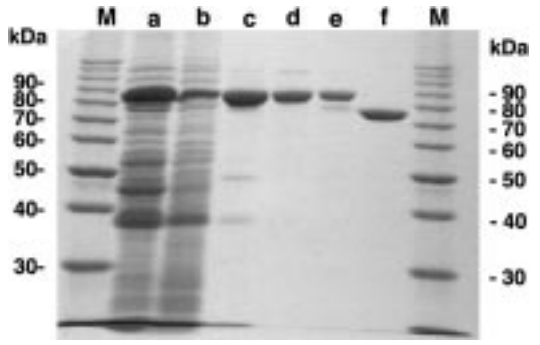

FIGURE 1: Purification of FpvA. Proteins from *P. aeruginosa* strains K691(pPVR2) (lanes a−d and f) and CDC5(pPVR2) (lane e) were resolved by SDS−PAGE (10% gel) and stained with Coomassie brillant blue. Key for lanes: M, molecular weight marker; a, outer membranes; b, soluble fraction after Zwittergent 3-14 treatment; c, after the first anion exchange chromatography at pH 8.0; d−f, after anion exchange chromatography at pH 6.8; f, FpvA migrates as a lower MW band when purified in the absence of protease inhibitors.

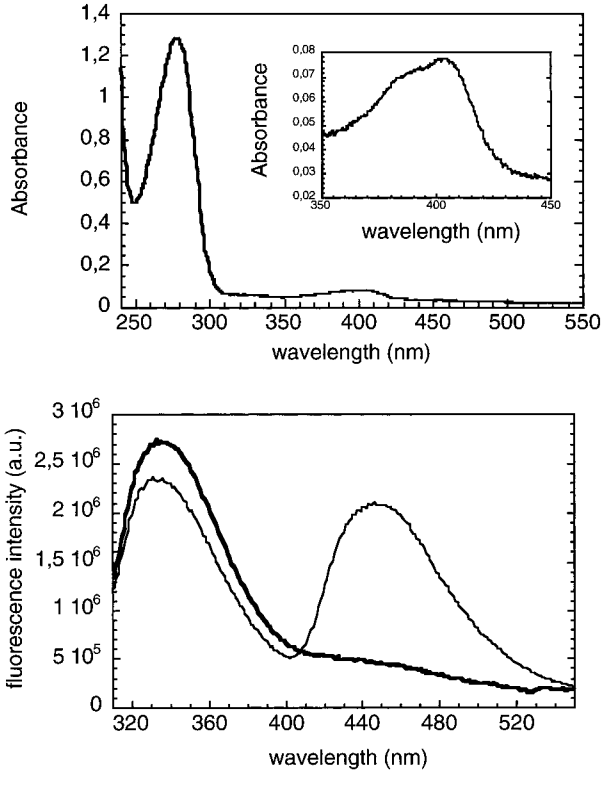

FIGURE 2: UV and fluorescence spectra of purified FpvA and FpvA−X. (A) UV spectra of FpvA−X. The enlargement of the FpvA−X spectrum from 350 to 450 nm (inset) shows a clear maximum of absorption at 400 nm which is absent in the FpvA spectrum (not shown). (B) Fluorescence spectra. Note that the emission maximum at 447 nm with FpvA−X (thin line) is absent with FpvA (thick line). The excitation wavelength was set at 290 nm. Proteins were dissolved in 50 mM Tris-HCl pH 8.0 and 1% (v/v) octyl-POE.

of 290 nm, ligand X was excited by energy transfer via the tryptophans of FpvA. The copurified ligand X could be excited directly at 400 nm, also with an emission peak at 447 nm (spectrum not shown). No evidence for such copurification was observed by UV or fluorescent measurements when FpvA was purified from the PaA−deficient strain CDC5(pPVR2) (Figure 2B). It is interesting to note that under none of the various steps of the purification

Table 1: Characteristics of X, Pa and PaA

	X	PaA	PaA−Fe
UV (λ_{max}) 50 mM pyridine− acetic acid pH 5.0	360 nm 380 nm	360 nm 380 nm	400 nm 450 nm
fluorescence (λ_{max}) excitation 400 nm	460 nm	460 nm	not fluorescent
electrophoretic migration dist on cellulose acetate membranes	15 mm	15 mm	6 mm
HPLC C18 (retention time)	22 min[a]	18 min	22 min
mass spectrometry	1387 Da	1334 Da	1387 Da
mass spectrometry after acetic acid treatment	1334 Da		1334 Da

[a] X migrates as PaA−Fe most probably because iron loading occurs on the HPLC column as judged also from the shift in UV absorption maxima after purification by HPLC.

process (dialysis, chromatography) did molecule X dissociate or separate from FpvA.

Purification and Characterization of the Ligand X Copurified with FpvA. Ligand X was tightly bound to FpvA and could be only removed from the receptor using harsh conditions (e.g. urea, strong acidic medium). To characterize the copurified ligand X, purified FpvA−X from the PaA-producing strain K691(pPVR2) was denatured at pH 2.0 by the addition of TFA (trifluoroacetic acid). This denaturation was monitored by fluorescence spectra measurements (excitation at 290 nm) where the observed tryptophan emission peak shifted from 337 to 350 nm and the ligand X emission peak at 447 nm disappeared (emission spectra not shown). FpvA−X denaturation at pH 2.0 led to a decay of the energy transfer between the tryptophans of FpvA and the copurified ligand X. Molecule X was then separated from denatured FpvA by filtration on a centricon, and the separation was monitored by UV or by fluorescence (excitation 400 nm) spectra measurements.

Table 1 compares the features of ligand X, PaA, and PaA−Fe. At pH 5.0, X had a λ_{max} at 360 and 380 nm typical of PaA (*5*). In 50 mM pyridine−acetic acid pH 5.0, the addition of iron to X transformed the spectrum to one typical of pyoverdin−Fe(III) complexes, exhibiting a λ_{max} at 400 and a shoulder at 450 nm (*27, 34*; Table 1). When excited at 400 nm, X had a fluorescence emission maximum at 460 nm, exactly as for PaA, and this was abolished upon iron complexation (Table 1). Similarly, the electrophoretic migration distance of ligand X on cellulose acetate membranes was the same as for PaA (15 mm; Table 1). To determine the molecular mass of ligand X by mass spectrometry, X was further purified by HPLC using the PaA purification protocol (*6, 7*). During this HPLC purification, X captured iron from the column and formed an X−Fe complex with the same retention time as PaA−Fe (Table 1). Mass spectrometric measurements gave a mass of 1387 Da for X−Fe in agreement with the mass determined for PaA−Fe under the same conditions. After acetic acid treatment of X-Fe, a mass of 1334 Da was measured, identical to the mass determined for apo-PaA under the same conditions (Table 1).

From these data, it was possible to clearly identify X as iron-free PaA. Furthermore, the titration of X with an iron(III) solution according to Meyer and Abdallah (*27*) showed a 1:1 stoichiometry (data not shown).

Binding Characterization of FpvA. As shown in Figure 3A purified FpvA from strain CDC5(pPVR2) binds PaA−^{55}Fe in a saturable manner with a dissociation constant of 14 ± 4 nM (n = 5) derived from Scatchard analysis. This K_d value is consistent with the K_i value deduced from the

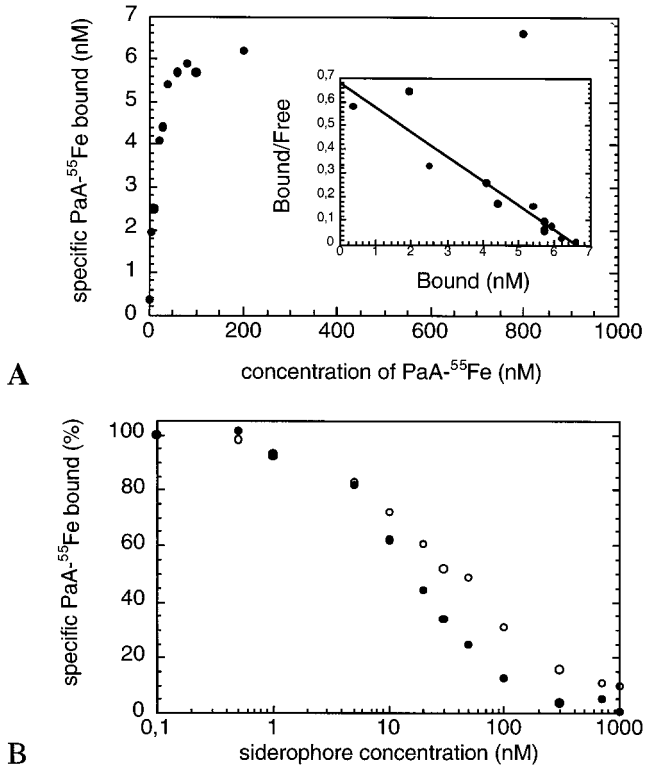

FIGURE 3: (A) Saturation curve and Scatchard analyzes for the binding of PaA−^{55}Fe to purified FpvA. Binding assays were performed as described in Materials and Methods. Purified FpvA from strain CDC5(pPVR2) (8 nM) was incubated for 2 h at room temperature in the presence of different concentrations of PaA−^{55}Fe in 50 mM Tris-HCl pH 8.0 and 1% (v/v) octyl-POE. Each point is the average of triplicate determinations. Inset: Scatchard analyses of specific binding. (B) Competition by unlabeled PaA−Fe and iron-free PaA for the binding of PaA−^{55}Fe to purified FpvA. Experiments were performed as described in Materials and Methods in the presence of 8 nM purified FpvA from strain CDC5(pPVR2), 12 nM PaA−^{55}Fe, and various concentrations of PaA (○) and PaA−Fe (●). Results are expressed as the percentage of the specific PaA−^{55}Fe binding. Each point is the average of triplicate determinations. Experiments were repeated two times with comparable results.

typical displacement binding experiments (Figure 3B). A 12 nM concentration solution of PaA−^{55}Fe was used to incubate purified FpvA together with various concentrations of nonlabeled ferric−PaA or iron-free PaA. The nonradioactive concentrations at which a 50% maximal specific binding was observed (IC_{50}) for FpvA were estimated to be 30 and 15 nM respectively for apo-PaA and PaA−Fe. The K_i (Materials and Methods) can therefore be calculated to be 17 and 8 nM respectively for apo-PaA and PaA−Fe. The comparison of the binding constants calculated above for PaA−Fe and apo-PaA to FpvA shows no significative difference between the affinities of these two forms of PaA to FpvA. These

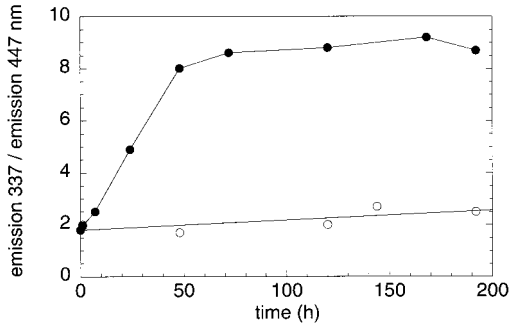

FIGURE 4: Formation of iron-loaded FpvA−PaA. Purified FpvA−PaA from PaA producing strain K691(pPVR2) was incubated for different lengths of time in the presence of 70 μM PaA−Fe (●) or 1 mM citrate-Fe (○) as described under Materials and Methods. After incubation, the protein was separated from unbound PaA−Fe or citrate−Fe and the percentage of ferric FpvA−PaA formed calculated as described in Materials and Methods.

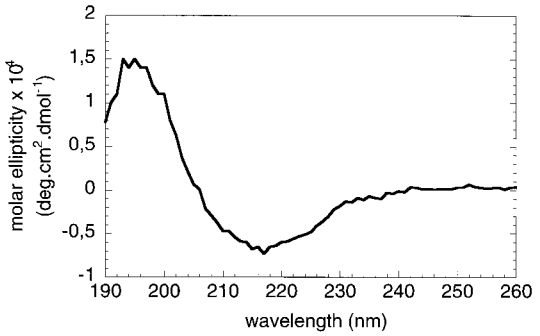

FIGURE 5: Far-UV circular dichroism spectra of purified FpvA. The purified FpvA protein (2.1 μM) was solubilized in 50 mM potassium phosphate buffer pH 6.8 and 1% (v/v) octyl-POE. Measurements were carried out at 24 °C over an optical pathway of 0.02 cm.

binding data for iron-free PaA are fully consistent with the copurification described above and indicates that the purified FpvA retains its binding activity and specificity after detergent extraction and purification.

The saturable binding of iron free PaA to FpvA could also be followed by fluorescence resonance energy transfer measurements between the tryptophans of FpvA and apo-PaA when excited at 290 nm (data not shown). Purified FpvA from strain CDC5(pPVR2) had only one emission peak which occurred at 337 nm and corresponded to the tryptophan fluorescence (Figure 2B). When the protein binds iron-free PaA, a second peak of fluorescence emission appeared at 447 nm reflecting the energy transfer between FpvA and apo-PaA, acting, therefore, as an indicator of binding. In theory, the fluorescence resonance energy transfer between FpvA and apo-pyoverdin can be used to determine the binding constants for apo-PaA and ferric−PaA to its receptor. However, for technical reasons (sensitivity, direct ligand excitation) a concentration of FpvA of at least 150 nM had to be used. This protein concentration is too high compared to the affinity of apo-PaA to FpvA (17 nM according to the displacement experiment described above with PaA−^{55}Fe) to avoid ligand depletion and therefore may lead to erroneous interpretation of ligand association data when the Scatchard plot is used.

Formation of an Iron-Loaded FpvA−PaA Form: FpvA−PaA−Fe. To determine if FpvA−PaA was able to complex iron in vitro, FpvA−PaA purified from the PaA-producing strain K691(pVR2) was incubated for different lengths of time in the presence of PaA−Fe or citrate−Fe as described in the Materials and Methods. After incubation, the protein was separated from unbound PaA−Fe or from citrate−Fe by gel filtration (which did not dissociate ligand from FpvA) and the ratio of the fluorescence emission at 337 nm to the emission at 447 nm was calculated after excitation at 290 nm. As shown in Figure 2B, when excited at the excitation wavelength of the tryptophans (290 nm), FpvA−PaA was characterized by two emission peaks at 337 and 447 nm. Since the PaA−Fe complex is not fluorescent, the formation of the iron-complexed form of FpvA−PaA could be visualized by the disappearance of the emission peak at 447 nm.

Figure 4 shows a very slow FpvA−PaA−Fe complex formation when purified FpvA−PaA was incubated in the presence of PaA−Fe. From this experiment it was not possible to determine whether purified FpvA−PaA was binding the iron ion of PaA−Fe or whether there was an exchange between the FpvA-bound PaA and PaA−Fe. In the presence of an excess of PaA−Fe, the saturation plateau of the protein−siderophore−iron complex formation was reached only after 50 h incubation at room temperature. The kinetic of formation of FpvA−PaA−Fe when PaA-free FpvA is incubated in the presence of PaA−Fe is much faster (results not shown). Indeed, the saturation plateau of the FpvA−PaA−Fe complex formation was reached in less than 15 min.

No significant iron complexation was observed when purified FpvA−PaA was incubated in the presence of 1 mM citrate−Fe, even after 8 days of incubation. We have shown that PaA alone in solution was able to complex iron from citrate−Fe in a few seconds at pH 5.0 (results not shown). From the results described in Figure 4, it was not possible to conclude whether purified FpvA−PaA was unable to chelate iron when citrate was the donor or if the kinetics of chelation were much slower than when PaA−Fe was the iron donor. Bates and Werniche (*35*) have shown that transferrin chelates iron with different kinetics depending on the iron donor. Transferrin chelates iron in a few seconds from ferric nitrilotriacetic acid, in 20 h from citrate−Fe and in 6 days from EDTA.

Circular Dichroism (CD) Spectral Analysis of FpvA. The secondary structure of purified FpvA was assessed from the CD far-UV spectrum obtained in 50 mM potassium phosphate buffer pH 6.8 and 1% (v/v) octyl-POE at room temperature. The CD spectrum of FpvA displayed a negative band at 217 nm and a strong positive band at 195 nm (Figure 5) which is characteristic of a high β-sheet content (reviewed in ref *36*). Deconvolution of the spectrum using the CONTIN program (*32*) indicated 57% β-structure, 3% α-helix, and 40% random coil, values almost identical to those obtained for the *E. coli* porin OmpF (58% β-structure, 8% α-helix, and 34% random) using the same spectropolarimeter and deconvolution program or from the X-ray coordinates of OmpF (58% β-sheet, 4.5% α-helices and 37.5% remainder). These data are also comparable to the CD values published for FhuA (*37, 38*) and consistent with the X-ray structures of FhuA (*14, 15*) and FepA (*16*); respectively the ferrichrome and the enterobactin outer membrane receptors from *E. coli*.

Purification of a Proteolyzed Form of FpvA−PaA. The presence of the protease's inhibitors (cocktail tablets) was

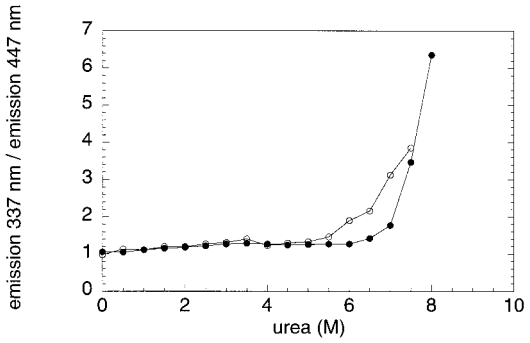

FIGURE 6: Urea denaturation of FpvA−PaA and tFpvA−PaA. The ratio of emission at 337 nm to the emission at 447 nm was measured at various urea concentrations for FpvA−PaA (●) and tFpvA−PaA (○).

necessary during the purification of FpvA to avoid the formation of a truncated form of FpvA (called tFpvA) or FpvA−PaA (called tFpvA−PaA) (Figure 1). The molecular mass as determined by mass spectrometry (MALDI-MS) yielded 77 177 ± 1025 Da for the proteolyzed form and 86 109 ± 1167 Da for the full length protein. N-terminal micro sequencing of the 77 kDa species revealed a sequence $_{88}$MITSNQLGTI$_{97}$ that was matched to the primary sequence of FpvA (*12*). From the molecular mass and the N-terminal sequence it could be concluded that the C-terminus of tFpvA was intact and that cleavage occurred only at the N-terminus. The CD spectra of tFpvA−PaA in the far UV showed that tFpvA−PaA remains a β-sheet protein (data not shown). Fluorescence measurements (excitation set at 290 nm) of tFpvA−PaA purified from the PaA-producing strain K691-(pPVR2) indicated that this truncated protein still bound apo-PaA (emission spectra not shown). Figure 6 shows the effect of urea on the ratio of emission at 337 nm to the emission at 447 nm for FpvA−PaA and tFpvA−PaA. When the protein started to be denatured in 7 M urea, apo-PaA was no longer able to be excited by energy transfer via the tryptophans, yielding a decrease in the emission peak at 447 nm and an increase of the ratio calculated in Figure 6. It is clear, therefore, that the absence of the 87 N-terminal amino acids did not destabilize tFpvA−PaA and did not affect the binding of apo-PaA to the receptor.

DISCUSSION

In this paper we describe the successful purification and characterization of FpvA, the ferric pyoverdin receptor, from two *P. aeruginosa* strains, one producing PaA [K691-(pPVR2)] and one unable to produce PaA [CDC5(pPVR2)]. Surprisingly, the characterization of purified FpvA expressed in strain K691(pPVR2) by UV and fluorescence spectroscopy revealed a copurification of FpvA with iron-free PaA. Royt (*39*) described a membrane associated iron chelator (MAIC) extracted with ethanol from the inner membranes of *P. aeruginosa*. The UV spectra described for this MAIC molecule is completely different from the one described here for PaA copurified with FpvA. The energy transfer observed between the copurified iron-free PaA and the FpvA tryptophans (Figure 2B) indicated that apo-PaA is located within a binding pocket of the protein at a short distance from tryptophans. Using the molecular extinction coefficient of FpvA at 280 nm and of apo-PaA at 380 nm, we could estimate that 100% of the purified FpvA from strain K691

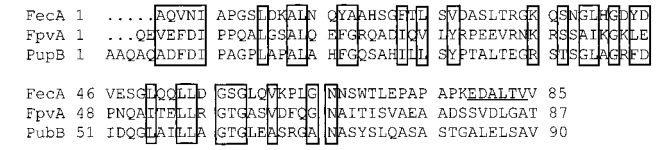

FIGURE 7: Sequence comparison of the N-terminal extension of FpvA with PubB from *P. putida* and FecA from *E. coli*. Identical or strongly similar regions are boxed. The proposed TonB box from FecA is underlined (*44*).

contained a molecule of apo-PaA in its binding site. In other words, iron-free PaA binds to FpvA with a stoichiometry of 1:1. Similarly, one molecule of ferric siderophore per molecule of receptor has been calculated for FepA and FhuA, two siderophore outer membrane receptors of *E. coli* (*40*, *41*). The CD spectrum of FpvA in the far UV indicates that the protein belongs to the β-barrel class of membrane proteins as the porins (see results, Figure 5) and as the siderophore outer membrane receptors FhuA and FepA (*14*−*16*).

When purification of FpvA−PaA was carried out in the absence of protease inhibitors, a truncated form of FpvA−PaA lacking the first 87 N-terminal amino acids (tFpvA−PaA) was obtained. tFpvA−PaA is as stable as FpvA−PaA as judged from urea denaturation curves (Figure 6), it retained pyoverdin binding ability, and its far UV CD spectrum and β-sheet content was comparable to that of the native form (data not shown). These results imply that the first 87 amino acids do not contribute to the β-barrel structure, and they are consistent with the 3D structures of FhuA and FepA (*14*−*16*). This stretch of amino acids may be part of a long periplasmic extension as predicted for the FecA ferric citrate receptor of *E. coli* and the PupB ferric pseudobactin receptor of *Pseudomonas putida*. For these two receptors, this N-terminal extension in front of the tonB box has been shown to play a role in signal transduction and transcriptional control of iron transport genes probably by interacting with the signal transducer, a protein with a simar topology as the TonB protein (FecR for *E. coli* or its analogue in *P. putida*) (*42*−*45*). There is some evidence that pyoverdin positively regulates receptor gene expression (*13*), and there is a clear homology between the N-terminal sequence of the three receptors (Figure 7, 30% and 23% identity, 51% and 53% similarity to PupB and FecA, respectively). This supports the hypothesis that FpvA possesses as well a periplasmic N-terminal with the same signal transduction function.

To our knowledge, copurification of a siderophore receptor with bound iron-free siderophore has never been reported, and no other data are available on the binding of metal-free siderophores to cells, outer membranes, or purified siderophore receptors. Guterman (*46*, *47*) has noted that iron−free enterobactin, the siderophore produced by *E. coli*, is an inhibitor of the action of protein antibiotic colicin B in *E. coli*. In contrast to the results of Guterman, Pugsley and Reeves (*48*) have shown that iron-free enterobactin is a much less effective inhibitor of colicin action than ferric enterobactin. In our case, it is interesting to note that the energy transfer between apo-PaA and the tryptophans of FpvA was also clearly detectable using outer membrane preparations prepared from strain K691(pPVR2) (data not shown). This suggests that iron-free PaA is already bound to FpvA on the surface of the cells and that this copurification may not be an artifact of the purification protocol. Moreover, in vitro,

purified FpvA from strain CDC5(pPVR2) is able to bind apo-PaA or the PaA−Fe complex in a saturable fashion with equivalent affinities (Figure 3) and purified FpvA−PaA from strain K691(pPVR2) can be loaded with iron upon incubation with PaA−Fe (Figure 4). This strongly suggests that the two forms of purified FpvA (FpvA and FpvA−PaA) are functional, at least as regards to ligand binding. PaA−Fe binds purified FpvA with a dissociation constant of 14 nM ± 4 ($n = 5$) which is consistent with the values described for other ferric siderophores for their receptors in intact cells or in vitro (*40*, *49*, *50*). Locher and Rosenbush (*41*), using experimental conditions ignoring ligand depletion, described a probably underestimated affinity of iron−ferrichrome for FhuA (in the range of 50−100 nM).

The inhibition constant determined for iron free PaA to FpvA ($K_i = 17$ nM) raises questions about the iron transport mechanism in *P. aeruginosa*. Indeed, as with other siderophore-producing Gram-negative bacteria, *P. aeruginosa* produces and excretes siderophores in the extracellular medium under iron-limited conditions. If the uptake mechanism is identical to the one proposed for other siderophores such as ferrichrome, after iron complexation, PaA−Fe binds to FpvA and is transported through the outer membrane via FpvA in a TonB-dependent process, dependent also, upon an energized cytoplasmic membrane. In the medium under iron limitation, the free form of the siderophore is always in excess relative to the iron-loaded siderophore. Thus, it is difficult to conceive how an efficient iron uptake mechanism can cope with a receptor which has the same affinity for iron-loaded and iron-free siderophore.

Binding of apo-PaA or PaA−Fe complex to FpvA is relatively fast and is complete within less than 15 min under our experimental conditions, suggesting that the FpvA binding site is accessible to its ligand. Irrespective of how the FpvA−PaA complex was formed (purification of the preformed complex from a pyoverdin producing strain or incubation of apo-PaA with the PaA free form of the receptor), it is extremely stable, and dissociation could be obtained only under denaturing conditions. These observations argue in favor of a slow k_{off} for iron-free PaA from FpvA. These results imply that since, under iron limitation, *P. aeruginosa* produces pyoverdin in excess relative to iron and FpvA, a FpvA−PaA complex forms initially in the outer membrane and this complex would not be able to transport iron into the periplasm efficiently unless a cofactor is present or a triggering mechanism is activated. Since this stable FpvA−PaA complex is also present in outer membrane preparations, the cofactor is probably a periplasmic protein. The best candidate cofactor is the protein TonB, and there is evidence that iron-loaded siderophores promote the interaction of FhuA and FepA with TonB (*51*−*53*). Whether iron-free siderophores also promote this interaction has not been investigated. We predict that, in order to get efficient iron uptake under iron limitation, the FpvA−PaA receptor in the outer membrane should interact with a cofactor, probably TonB, to trigger either fast iron loading of the already bound pyoverdin or pyoverdin exchange with iron-loaded siderophores from the external medium. This is different from the current view that TonB triggers a conformational change to release bound ferric siderophore inside the periplasm. Under our hypothesis TonB-dependent energy coupling will also be necessary in the earlier step of iron-binding to the receptor.

It is not clear yet wether this proposed mechanism and the high affinity binding of the apo-siderophore to its receptor may be a common feature of all siderophore receptors or whether this is a unique property of the subclass of receptors involved in signal transduction (FpvA, FecA, PubB) which possess an additional N-terminal extension. As described above FpvA may act as the ferric citrate receptor FecA for which siderophores in the growth medium trigger transcriptional activation of genes. For this class of receptors apo-siderophore binding (retention) to the receptor may be involved in this process.

Clearly, the mechanism of iron transport via FpvA−PaA across the outer membrane remains an open question and certainly additional data for FpvA and other ferric siderophore receptors are needed before any solid conclusions can be made.

ACKNOWLEDGMENT

We thank M.-P. Reck for her constant advice during the course of this work and O. Sorokin for carrying out the mass determination of the receptors. We thank Smith-Klyne-Beechham (Welwyn, Herts, U.K.) for generously providing carbenicillin.

REFERENCES

1. Cox, C. D., and Adams, P. (1985) *Infect. Immun. 48*, 130−138.
2. Cox, C. D., Rinehart, K. L., Moore, M. L., and Cook, J. C. (1981) *Proc. Natl. Acad. Sci. U.S.A. 78*, 4256−4260.
3. Griffiths, E. (1991) *Biol. Met. 4*, 7−13.
4. Cox, C. D., and Graham, R. (1979) *J. Bacteriol. 137*, 357−364.
5. Wendenbaum, S., Demange, P., Dell, A., Meyer, J. M., and Abdallah, M. A. (1983) *Tetrahedron Lett. 24*, 4877−4880.
6. Demange, P., Wendenbaum, S., Linget, C., Mertz, C., Cung, M. T., Dell, A., and Abdallah, M. A. (1990) *Biol. Met. 3*, 155−170.
7. Albrecht-Garry, A. M., Blanc, S., Rochel, N., Ocacktan, A. Z., and Abdallah, M. A. (1994) *Inorg. Chem. 33*, 6391−6402.
8. Braun, V. (1995) *FEMS Microbiol. Rev. 16*, 295−307.
9. Bradbeer, C. (1993) *J. Bacteriol. 175*, 3146−3150.
10. Postle, K. (1993) *J. Bioenerg. Biomembr. 25*, 591−601.
11. Poole, K., Neshat, S., and Heinrichs, D. (1991) *FEMS Microbiol. Lett. 78*, 1−5.
12. Poole, K., Neshat, S., Krebes, K., and Heinrichs, D. E. (1993) *J. Bacteriol. 175*, 4597−4604.
13. Gensberg, K., Hughes, K., and Smith, A. W. (1992) *J. Gen. Microbiol. 138*, 2381−2387.
14. Ferguson, A. D., Hofman, E., Coulton, J. W., Diederichs, K. and Welte, W. (1998) *Science 282*, 2215−2220.
15. Locher, K. P., Rees, B., Koebnik, R., Mitschler, A., Moulinier, L., Rosenbush, J. P., and Moras, D. (1998) *Cell 95*, 771−778.
16. Buchanan, S. K., Smith, B. S., Venkatramani, L., Xia, D., Esser, L., Palnitkar, M., Chakraborty, R., van der Helm, D., and Deisenhofer, J. (1999) *Nat. Struct. Biol. 6*, 56−63.
17. Liu, J., Rutz, J. M., Klebba, P. E., and Feix, J. B. (1994) *Biochemistry 33*, 13274−13283.
18. Jiang, X., Payne, M. A., Cao, Z., Foster, S. B., Feix, J. B., Newton, S. M. C., and Klebba, P. E. (1997) *Science 276*, 1261−1264.
19. Ankenbauer, R., Hanne, L. F., and Cox, C. D. (1986) *J. Bacteriol. 167*, 7−11.

20. Ausubel, F. M., Brent, R., Kingston, R. E., Moore, D. D., Seidman, J. G., Smith, J. A., and Struhl, K. (1992) in *Short protocols in molecular biology*, 2nd ed., J. Wiley and Sons, Inc., New York.
21. Dean, C. R., and Poole, K. (1993) *Mol. Microbiol. 8*, 1095−1103.
22. Simon, R., Priefer, U., and Puehler, A. (1983) *Biotechnology 1*, 784−791.
23. Fellay, R., Frey, J., and Krisch, H. (1987) *Gene 57*, 147−154.
24. Demange, P., Wendenbaum, S., Bateman, A., Dell, A. and Abdallah, M. A. (1987) in *Iron transport in microbes, plants and animals* (Winkelmann G., van der Helm, D., and Neilands, J. B., Eds.) pp 167−187, VCH Verlagsgesellschaft, Weinheim, Germany.
25. Mizuno, T., and Kageyama, M. (1978) *J. Biochem. 84*, 179−191.
26. Hancock, R. E. W., and Nikaido, H. (1978) *J. Bacteriol. 136*, 381−390.
27. Meyer, J. M., and Abdallah, M. A. (1978) *J. General. Microbiol. 107*, 319−328.
28. Simon, J., Benythe, S., Hepp, J., Kahn, A., Borsodi, A., Szücs, M., Medzihradsky, K., and Wolleman, M. (1987) *Neuropeptides 10*, 19−28.
29. Simon, J., Benythe, S., Hepp, Varga, E., Medzihradsky, K., Borsodi, A., and Wolleman, M. (1990) *J. Neurosci. Res. 25*, 549−555.
30. Ohtaki, T., Ogi, K., Masuda, Y., Mitzuoka, K., Fujiyoshi, Y., Kitada, C., Sawada, H., Onda, H., and Fujino, M. (1998) *J. Biol. Chem. 273*, 15464−15473.
31. Cheng, Y. C., and Prusoff, W. H. (1973) *Biochem. Pharmacol. 22*, 3099−3108.
32. Provencher, S. W., and Glöckner, J. (1981) *Biochemistry* 20, 33−37.
33. Manaval, P., and Johnson, W. C., Jr (1987) *Anal. Biochem. 167*, 76−85.
34. Abdallah, M. A. (1991) in *Handbook of Microbiol Iron Chelates* (Winkelman, G., Ed.) CRC Press Inc., Boca Raton, FL.
35. Bates, G. W., and Wernicke, J (1971) *J. Biol. Chem. 246*, 3679−3695.
36. Woody, R. W. (1995) *Methods Enzymol. 246*, 34−71.
37. Boulanger, P., le Maire, M., Bohnivers, M., Dubois, S., Desmadril, M., and Letellier, L. (1996) *Biochemistry 35*, 14216−14224.
38. Moeck, G. S., Bazzaz, S. F., Gras, M. F., Ravi, T. S., Ratcliff, M. J. H., and Coulton, J. W. (1996) *Mol. Microbiol. 22*, 459−471.
39. Royt. P. W. (1988) *Biochim. Biophys. Acta 939*, 493−502.
40. Payne, M. A., Igo, J. D., Cao, Z., Foster, S. B., Newton, S. M. C., and Klebba, P. E. (1997) *J. Biol. Chem. 272*, 21950−21955.
41. Locher, K. P., and Rosenbush, J. P. (1997) *Eur. J. Biochem. 247*, 770−775.
42. Härle, C., Kim, I., Angerer, A., and Braun, V. (1995) *EMBO J. 14*, 1430−1438.
43. Venturi, V., Weisbeek, P., and Koster, M. (1995) *Mol. Microbiol. 17*, 603−610.
44. Kim, I., Stiefel, A., Plantor, S., Angerer, A., and Braun, V. (1997) *Mol. Microbiol. 23*, 333−344.
45. Koster, M., van Klompenburg, W., Bitter, W., Leong, J., and Weisbeek, P. (1994) *EMBO J. 13*, 2805−2813.
46. Guterman, S. K. (1971) *Biochem. Biophys. Res. Commun. 44*, 1149−1155.
47. Guterman, S. K. (1973) *J. Bacteriol. 114*, 1217−1224.
48. Pugsley, A. P., and Reeves, P. (1976) *J. Bacteriol. 127*, 218−228.
49. Zhou, X. H., van der Helm, D., and Adjimani, J. (1993) *BioMetals 6*, 25−35.
50. Newton, S. M. C., Allen, J. S., Cao, Z., Qi, Z., Jiang, X., Sprengel, C., Igo, J. D., Foster, S. B., Payne, M. A., and Klebba, P. E. (1997) *Proc. Natl. Acad. Sci. U.S.A. 94*, 4560−4565.
51. Skare, J. T., Ahmer, B. M. M., Seachord, C. L., Darveau, R. P., and Postle, K. (1993) *J. Biol. Chem. 268*, 16302−16308.
52. Letain, T. E., and Postle K. (1997) *Mol. Microbiol. 24*, 271−283.
53. Moeck, G. S., Coulton, J. W., and Postle, K. (1997) *J. Biol. Chem. 272*, 28391−28397.

BI990421X